

SIMULTANEOUS CATALYTIC REDUCTION OF CHROMIUM (VI) AND DEGRADATION OF NAPHTHOL BLUE BLACK BY SnO_2 NANOPARTICLES

¹D. Venkatesh, ²K. Anbalagan

¹Research scholar, ²Professor

Department of Chemistry

Pondicherry University, Pondicherry 605014, India

Abstract

Simultaneous conversion of Cr (VI) to Cr (III) and degradation of Naphthol blue black have been investigated using SnO_2 nanoparticles prepared by facile, simple, co-precipitation technique from stannous chloride dihydrate ($\text{SnCl}_2 \cdot 2\text{H}_2\text{O}$) and co-precipitator dimethyl oxalate and characterized. The photocatalytic efficiency of *nano* SnO_2 was proven results that there was a synergistic behavior between the Naphthol blue black and conversion of Cr (VI) to Cr (III). In addition, mixture of Cr (VI) and Naphthol blue black (NBB) were selected as the mixed model pollutants and their influencing factors such as concentration of mixtures ($\text{K}_2\text{Cr}_2\text{O}_7 + \text{NBB}$), catalyst dosage, intensity of light sources (254 and 365 nm), pH were also studied systematically. At lower pH, the efficiency was significantly improved for organic dye and Cr (VI) to the mixture. Blank experiment (without catalyst) and surface adsorption indicates that NBB and Cr (VI) degrades and surface interaction at relatively low efficient and possible mechanism was also studied respectively.

Key words: nano SnO_2 , photocatalytic, Cr (VI), Naphthol Blue Black.

1. INTRODUCTION

In recent years, water pollution is one of the most serious threaten to human health risks and which causes serious effect to humanity and eco-system [1]. Heavy metals and stable organic effluents releasing from Industrial processes such as electroplating, paint making, leather tanning, has awakened the public concern over the last decade [2]. Chromium is common potent carcinogenic, mutagenic environmental pollutant, which classified as priority pollutants and commonly presented as Cr (VI) and Cr (III) in nature. While Cr (III) can be immobilized and thus become less bio-available, so the reduction of Cr (VI) to Cr (III) is highly desired [3, 4]. Naphthol blue black (NBB), a complex textile diazo dye, has a high photo- and thermal-stability. It is widely used in the textile industry for dyeing wool, nylon, silk and textile printing. Other industrial use includes coloring of soaps, anodized aluminum and casein, wood stains and writing ink preparation [5, 6]. Nano materials are unique in nature because of their mechanical, optical, electrical, catalytic and magnetic properties. Semiconductor photocatalysis have been proven redox reactions to be effective for detoxification of harmful pollutants in wastewaters [7, 8]. However, photocatalytic reduction Cr (VI) or oxidative degradation of dyes have investigated alone, very little attention focused to collectively treat the samples containing both Cr (VI) and dyes [9]. Among several semiconductors, tin oxide (SnO_2) is an n-type semiconductor with a wide band gap ($E_g \geq 3.6$ eV) at room temperature with rutile-tetragonal phase structure particularly pointed for its potential applications in microelectronics, gas sensing, protective coating, photovoltaic systems and photocatalysis [10]. The photogeneration of electron-hole pairs are well separated and slow recombination process by semiconductor nanostructures to enhance the photo-oxidation heavy metals and organic pollutants under ultraviolet region [11, 12].

Herein, SnO_2 nanoparticles prepared by a simple co-precipitation technique and synergistic effect on catalytic activity towards mixed model pollutants Cr (VI) and synthetic dyes (NBB) have been investigated in detail. Various control experiments were carried out such as concentration of mixtures (Cr (VI) + NBB), catalyst dosage, intensity of light sources (254 and 365 nm), pH were also studied. At pH 5 observed maximum efficiency of Naphthol blue black and catalytic conversion of Cr (III) under ultraviolet irradiation.

2. Experimental section

2.1 Materials and Methods

Potassium dichromate and Naphthol blue black were purchased from sigma-aldrich and used as model pollutants. *Nano* SnO_2 was prepared by a simple, facile, co-precipitation approach with some modifications [13] using stannous chloride dihydrate ($\text{SnCl}_2 \cdot 2\text{H}_2\text{O}$) and dimethyl oxalate. In a typical synthesis, 0.1 M of $\text{SnCl}_2 \cdot 2\text{H}_2\text{O}$ was dissolved in 10 mL 1-propanol under constant magnetic stirring for 10 min and to this 0.15 M of dimethyl oxalate in 10 mL of deionized water was added slowly over a period of 5 min. The resulting mixture was agitated for approximately 10 min and obtained precipitate was refluxed for a period of 24 h at ~

85 – 90 °C. Then it was cooled to room temperature, centrifuged, washed several times with 1:1 ratio of de-ionized water and ethanol (v/v). Finally, the precipitate was dried in oven at ~110 °C for 10 h and annealed for 3 h at 500 °C.

2.2 Characterization

The phase identification of the nanomaterial was characterized by powder X-ray diffraction (XRD; Bruker,) with Cu K α radiation ($\lambda = 1.5405 \text{ \AA}$). The morphology and microstructure of the synthesized sample were examined by scanning electron microscopy (SEM, JEOL JSM 6700F at 10kV) and high-resolution transmission electron microscopy (HRTEM, JEOL 2010 at 200 kV), The optical absorption characteristics are determined with UV-Vis absorbance spectra by using a Shimadzu, UV 2450 double-beam spectrophotometer equipped with integrating sphere attachment (ISR-2200).

2.3 Adsorption experiments

The surface adsorption experiments were carried out using Technico cooling water bath shaker at room temperature. 100 mg of SnO₂ nanoparticle was used as an adsorbent and slightly acidified aqueous medium 100 mL of potassium dichromate ($1.699 \times 10^{-4} \text{ M}$) and NBB ($2.703 \times 10^{-5} \text{ M}$) were taken in a 125 mL stoppered glass bottle performed. The adsorption of heavy metals and dye molecules were studied on the surface of catalyst at different time intervals (0, 5, 10, 20 and 30 min). The adsorbent was separated by centrifugation from their mixture, absorbance of potassium chromate and Naphthol blue black were characterized spectrally.

2.4 photocatalytic activity measurements

Catalytic degradation experiment was established by dispersing pure *nano* SnO₂ (100 mg) using model pollutants such as 100ml of K₂Cr₂O₇ ($1.699 \times 10^{-4} \text{ M}$) and NBB ($2.703 \times 10^{-5} \text{ M}$) in slightly acidified aqueous medium, then the solution was magnetically stirred in dark for 30 min at room temperature to establish adsorption-desorption equilibrium between the catalyst and mixtures. The experimental solution was then placed under UV light source (Heber Scientific, low pressure mercury vapor lamp, 6W, intensity measured; Light Meter, model: LX-1108, intensity of light of low pressure mercury lamp = 1800 lux) with maximum output at $\lambda = 254 \text{ nm}$. The temperature was kept close to room temperature by water circulating pump. Two-three milliliter aliquots from the photochemical reactor (quartz tube, capacity 100 mL, dia of inner-outer jacket = 0.5 cm) were withdrawn at definite time intervals (0, 5, 10, 20 and 30 min), centrifuged and spectrally analyzed ($\lambda_{\text{max}} \sim 251 \text{ nm}$ and 333 nm for Cr (VI), $\lambda_{\text{max}} \sim 619 \text{ nm}$ for NBB) to determine the concentration of chromium (VI) ions and NBB solution.

The degradation efficiency was estimated using the relationship: $[C_0 - C/C_0] \times 100$, where C₀ is the initial concentration and C at various time intervals. Further investigation of SnO₂ nanoparticles on the photodegradation process was made in presence of scavengers. 2-propanol (PrⁱOH) was added as the hydroxyl ($\cdot\text{OH}$) radical scavenger, p-benzoquinone as the superoxide ($\cdot\text{O}_2^-$) scavenger respectively.

3. Results and discussions

3.1 Structural Characteristics

Crystal phase identification was undertaken for the prepared *nano* SnO₂ shown in **Fig.1A**. All of the diffraction peaks for these samples could be well indexed as the tetragonal rutile phase (JCPDS File no. 41-1445). The peak positions $2\theta = 26.6, 33.9, 37.9, 51.780, 54.8, 57.8, 61.9, 64.7, 71.3$ correspond to the (110), (101), (200), (211), (220), (002), (310), (112), (202) lattice planes of tetragonal rutile SnO₂ [14]. The peaks are very sharp, intense showing high degree of crystallinity of the samples and no impurities were detectable. The average crystallite size of *nano* SnO₂ was calculated to be 18.4 nm using scherrer equation.

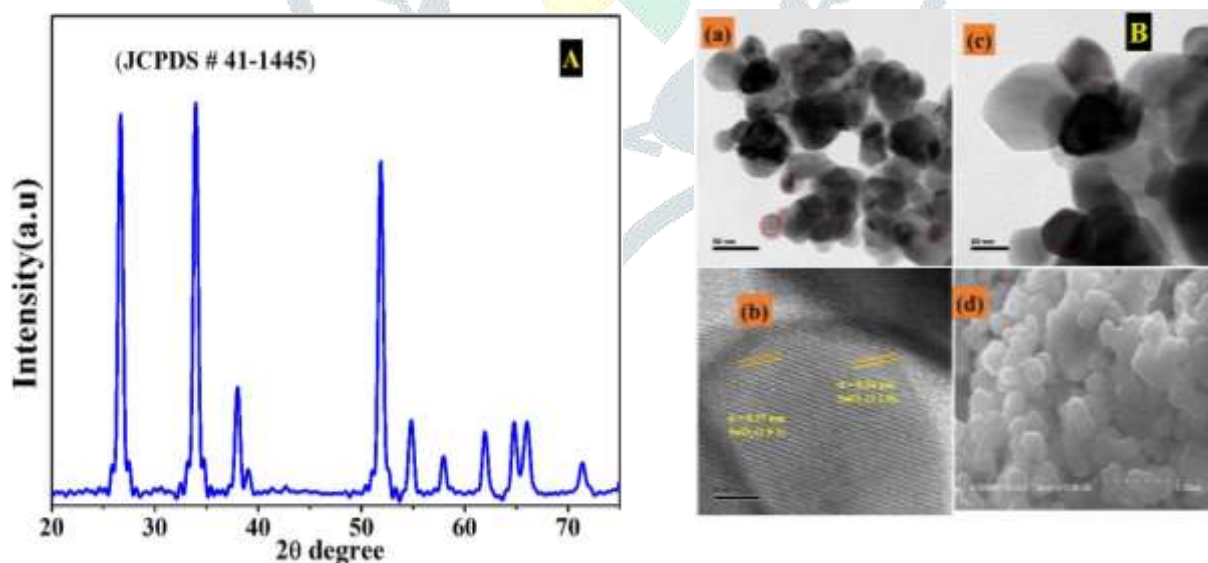


Fig. 1 (A) X-ray diffraction pattern of *nano* SnO₂ obtained from co-precipitation technique. **(B)** SEM and TEM micrographs

(a) TEM magnification (50 nm) micrographs of *nano* SnO₂ (b) inverse fast Fourier transform with indexing for relevant lattice spacing (c) 20 nm magnified micrograph (d) SEM micrograph (5 μm)

Fig.1B shown transmission electron microscopy (TEM) images at different magnified range 50nm and 20nm, inverse fast Fourier transform (IFFT) and SEM micrographs to confirm the size and morphology of the SnO₂ nanoparticles. The size of the SnO₂ was in the range between 18-26 nm and similar particle size results obtained in the XRD pattern. In **Fig.1** Ba, Bc, Bd TEM and SEM micrographs of tin oxide nanoparticles revealed that spherical shape with even particle distribution and slightly agglomerated

particles corresponding to tetragonal rutile tin oxide structure. In **Fig. 1. Bb** shows the IFET of SnO₂ inter planar distances of 0.35 and 0.26 nm correspond to the SnO₂ (110) and (101) low-index facets) are well matched (JCPDS 41-1445) to the rutile phase of SnO₂ [15].

3.2 Adsorption and Synergistic Photocatalytic Removal of Cr (VI) and NBB

In general, Surface adsorption of heavy metal and dye molecule contributes significantly for catalytic efficiency of the photocatalyst [16]. The adsorption-desorption process of Cr (VI) and NBB dye molecules on the surface of the nanoparticles closely approaches equilibrium within at 30 min. However, no significant changes are within this timescale. To this mixture, efficiency of surface adsorption was found to be 7 %, 26 % are observed at 30 min for chromium (VI) ions and 73% are observed for NBB at 30 min with catalyst quantity of 100 mg /100 mL at pH 5. Synergistic effect of photocatalytic reduction between Cr (VI) ions and NBB were tested using *nano* SnO₂ in slightly acidified aqueous medium and the track of time-dependent degradation and surface adsorption curves is presented in **Fig. 3a** and **3b**. Degradation efficiency of Cr (VI) and NBB with numerous optimum reaction conditions are presented in T1, T2, T3. The progression of the catalytic reduction and degradation dye of the mixture can be easily followed by the change in absorbance at $\lambda \sim 251$ nm and 333nm for Cr (VI) ions and $\lambda \sim 619$ nm for NBB. The absorbance decreases in the time dependent experiments and reduction of chromium (VI) ions and dye become colorless and without catalyst experiment were also tested, efficiency of experiments was low. In mixture, Naphthol blue black efficiency slightly increased strong sorption behavior at optimum level concentration.

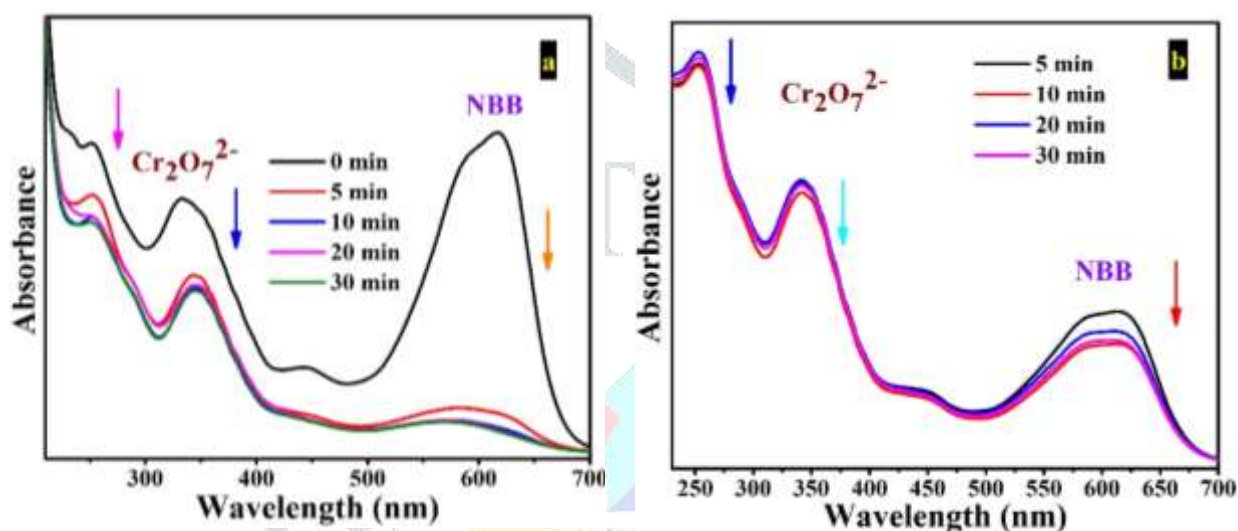


Fig. 3 (a) Time-dependent catalytic degradation and **(b)** surface adsorption of Cr₂O₇²⁻ ions and NBB solution (catalyst = 100 mg/100 mL) from the mixture at room temperature.

Mechanism

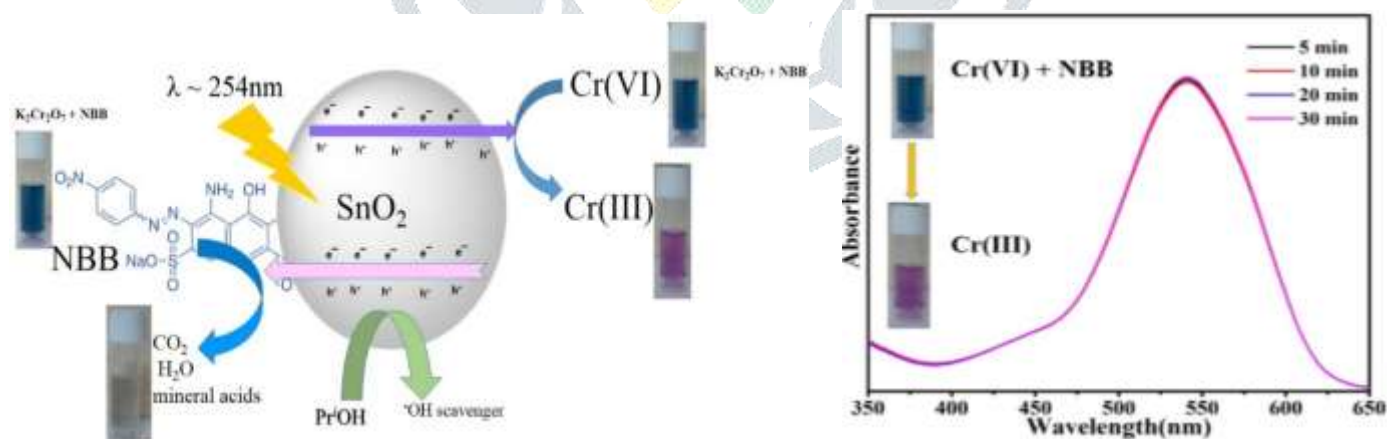


Fig. 4 Graphical representation of Cr (III) and NBB dye degradation pathways and spectral absorption during the conversion of Cr (III) monitoring for prepared catalyst at different time interval

The proposed photocatalytic mechanism and catalytic conversion of Chromium (III) ions are presented in **Fig.4**. Under ultraviolet irradiation, the valence band electrons of SnO₂ nanoparticles can be excited to conduction band and transfer the electron to hexavalent chromium ions. SnO₂ nanoparticles generates good separation electron-hole pairs and photogenerated reactive species involved to degrade the Cr(VI) and Naphthol blue black dye. Simultaneously, the organic dye and catalytic conversion of Cr (III) ion can be enhanced by the photogenerated hydroxyl ([•]OH) and superoxide ([•]O₂⁻) radicals respectively [17]. The formation of Cr (III) ions was measured during the photocatalytic reduction of Cr (VI) ions spectrophotometrically using the DPC (diphenylcarbazide) method as reported earlier [18]. An aliquot amount of 0.5 mL photolysed solution was added to a vial containing 2.5 mL of prepared DPC reagent (100 mL of D.I. water and 4 mL of DPC reagent that contains 5 mL of acetone, 50 μL

of H₂SO₄, and 0.01 g of DPC). The sample solution was mixed with reagent and kept for 30 minutes, measured spectrally. The absorbance measurements at 540 nm were done using a UV/visible spectrophotometer as presented with different time intervals.

3.3 Influencing Factors in Photocatalysis

Various controlled catalytic experiments carried out such as concentration of Cr (VI) and NBB dye molecules, quantity of the catalyst, pH, and intensity of the light sources.

Effect of Catalyst

Photocatalyst dosage enhancement allows more number of adsorption sites and provides more active sites for oxidative species formation ($\cdot\text{O}_2^-$, and $\cdot\text{OH}$) leading to a significant enhancement of the adsorbed dye molecules degradation rate [19]. The quantity of nano scale tin oxide was optimized by varying photocatalyst in the range 50-100 mg/100 mL for mixture K₂Cr₂O₇ as a Cr (VI) source and NBB dye in acidified aqueous medium. Fig. 5a, 5b and 5c depicted that, 100 mg in 100 mL of mixture yields maximum degradation rate was observed. The optimum catalyst density produces more number of photons and slow recombination process leads to electron/hole generation for the effective degradation of dye solution and catalytic conversion of Cr (III) so as to effectively reaching the surface of catalyst [20].

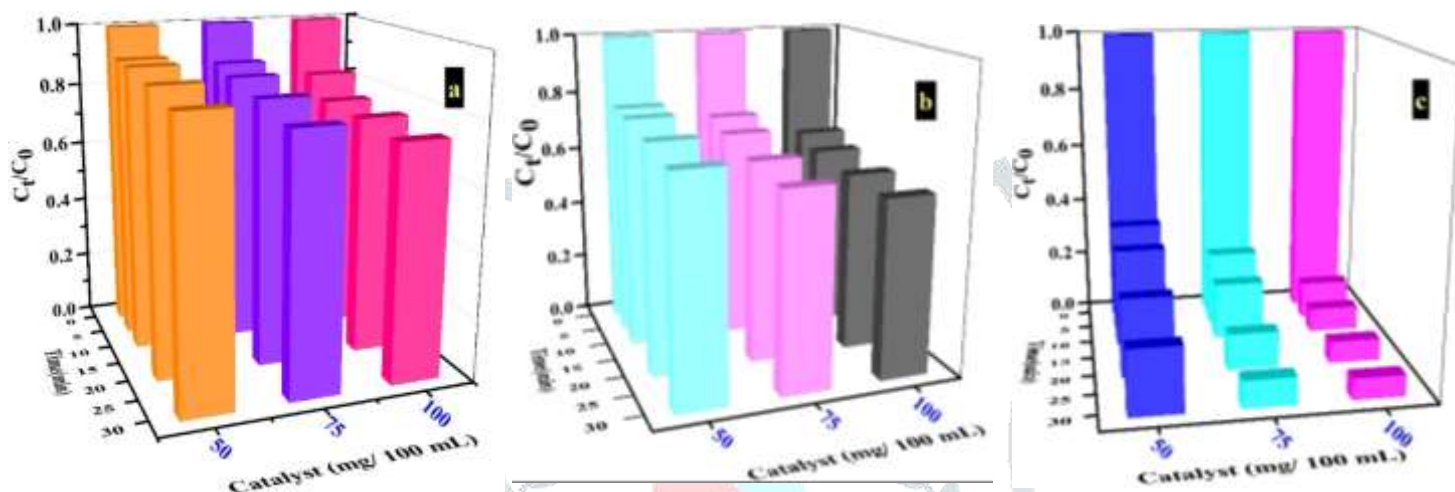


Fig. 5 Factors influencing photocatalytic degradation of K₂Cr₂O₇ as chromium (VI) source and Naphthol blue black from the mixtures. Effect of dosage at (a) Cr₂O₇²⁻ ($\lambda \sim 251$ nm) (b) Cr₂O₇²⁻ ($\lambda \sim 333$ nm) (c) NBB ($\lambda \sim 619$ nm).

Effect of Concentration

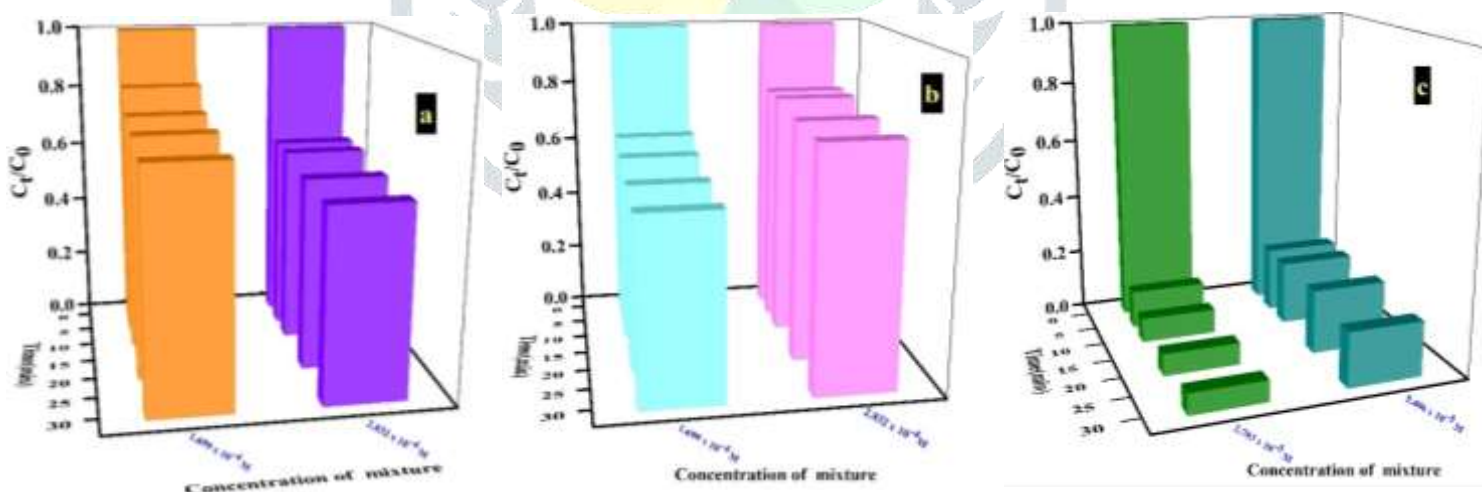


Fig. 6 Factors influencing photocatalytic degradation of K₂Cr₂O₇ as chromium (VI) source and Naphthol blue black from the mixtures. Effect of concentrations at (a) Cr₂O₇²⁻ ($\lambda \sim 251$ nm) (b) Cr₂O₇²⁻ ($\lambda \sim 333$ nm) (c) NBB ($\lambda \sim 619$ nm).

The concentration of mixture varied using K₂Cr₂O₇ (1.699 x 10⁻⁴ M - 2.832 x 10⁻⁴ M) and NBB (2.703 x 10⁻⁵ M - 5.406 x 10⁻⁵ M) have been investigated by constant catalyst loading 100 mg/100 mL and at pH 5 in aqueous medium. However, increase the concentration of mixture was doubled and catalytic conversion of Cr (VI) to Cr (III) and complete Naphthol blue black degradation efficiently at low concentration as a result of more available surface sites on the catalyst. At lower concentration, generation of more number of photogeneration radicals on the catalyst surface during dye degradation process [21]. Fig. 6a, 6b and 6c confirmed that at lower concentration more degradation rate was observed and higher concentration of mixed pollutants reduces the density of light source to reach the surface of the catalyst, degradation rate was also decreased for Cr₂O₇²⁻ ions and Naphthol blue black[22].

Effect of pH

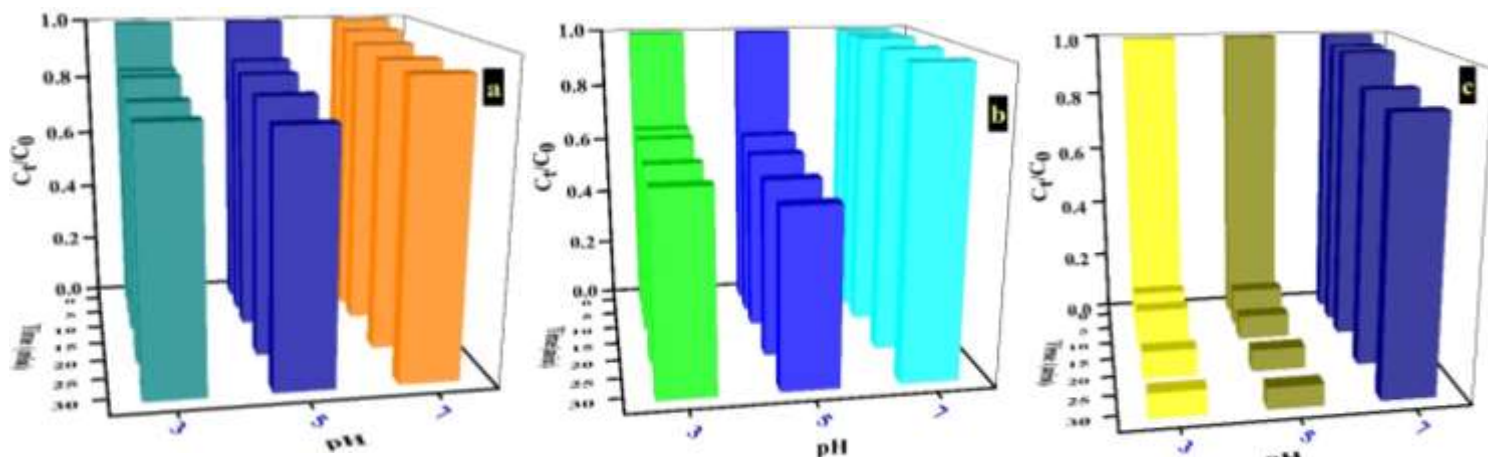


Fig. 7 Factors influencing photocatalytic degradation of $K_2Cr_2O_7$ as chromium (VI) source and Naphthol blue black from the mixtures. Effect of pH at (a) $Cr_2O_7^{2-}$ ($\lambda \sim 251$ nm) (b) $Cr_2O_7^{2-}$ ($\lambda \sim 333$ nm) (c) NBB ($\lambda \sim 619$ nm).

The pH of an aqueous medium can influence the photocatalytic process through absorption between dyes and the catalyst surface and redox processes of photocatalysts [23]. The photocatalytic experiments were performed at constant catalyst loading 100 mg nano SnO_2 in 100mL, the intensity of light sources (254 nm) with optimum concentration of mixture ($K_2Cr_2O_7 + NBB$) and the results were obtained by varying medium of the pH solution 3 to 7. **Fig. 7a, 7b** and **7c** revealed that, the maximum catalytic conversion of Cr (III) are 26 % ($\lambda \sim 251$ nm), 41 % ($\lambda \sim 333$ nm) and degradation rate for NBB (93 %) is achieved at pH = 5. At pH 3 slightly decreased the catalytic activity, more acidic medium of suspensions can be exaggerated on the surface charge of nanoparticles. The catalyst surface charge is negative evidenced increasing stronger electrostatic repulsion within the system and diminishing photogenerated oxidative species in the reaction [24]. In neutral medium, the interaction between the mixture and surface of the catalyst are not much achievable to enhance the photocatalytic activity of $Cr_2O_7^{2-}$ ions and Naphthol blue black.

Effect of Intensity of sources

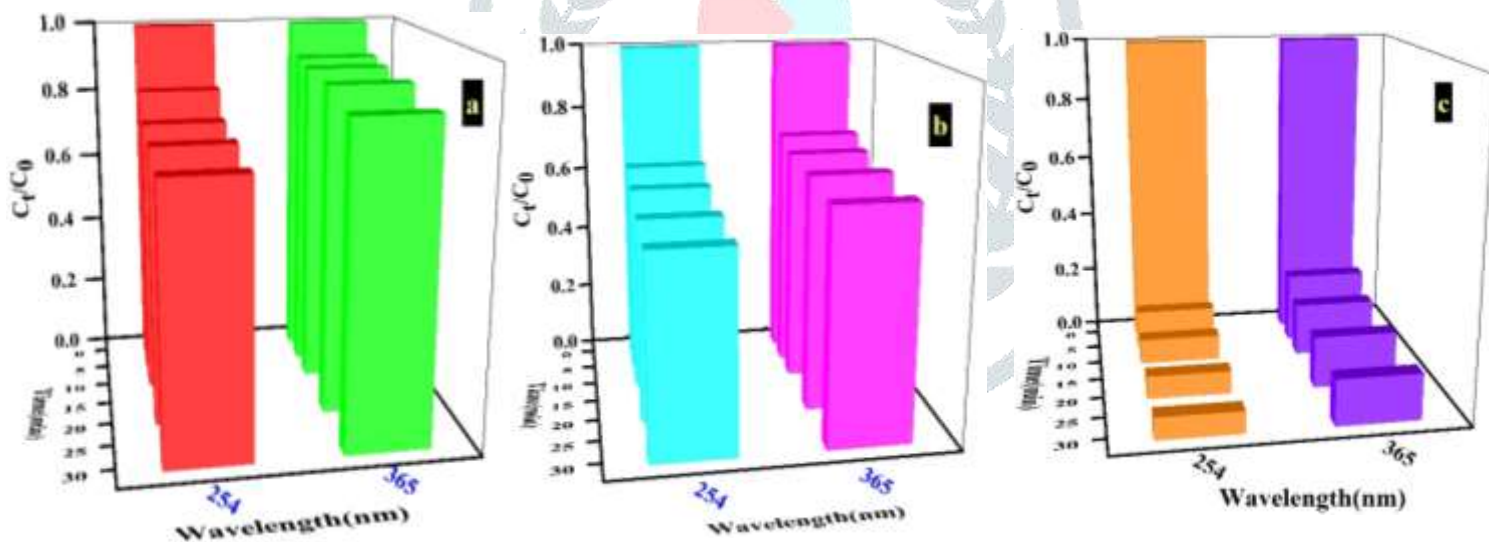


Fig. 8 Factors influencing photocatalytic degradation of $K_2Cr_2O_7$ as chromium (VI) source and Naphthol blue black from the mixtures. Effect of intensity of light sources at (a) $Cr_2O_7^{2-}$ ($\lambda \sim 251$ nm) (b) $Cr_2O_7^{2-}$ ($\lambda \sim 333$ nm) (c) NBB ($\lambda \sim 619$ nm).

Fig. 8a, 8b and **8c** showed that the degradation of mixtures (Cr (VI) + NBB) were performed constant catalyst loading 100 mg nano SnO_2 in 100mL with optimum concentration of mixture ($K_2Cr_2O_7 + NBB$) at pH 5 under 254 and 365 nm irradiation. It was observed that, catalytic conversion of Cr (III) ions and degradation rate of dye increased with 254 nm > 365 nm as given intensity of light source. In higher wavelength, the inability to generate more electrons-holes combination and oxidative species during the photocatalytic reactions to degrade the dye and catalytic conversion of Cr (III). This indicates that, more electrons and holes are produced per unit time and efficient reactive radical formation to degrade the dye molecules faster rate at lower wavelength [25].

3.4 Effect of radical scavenger

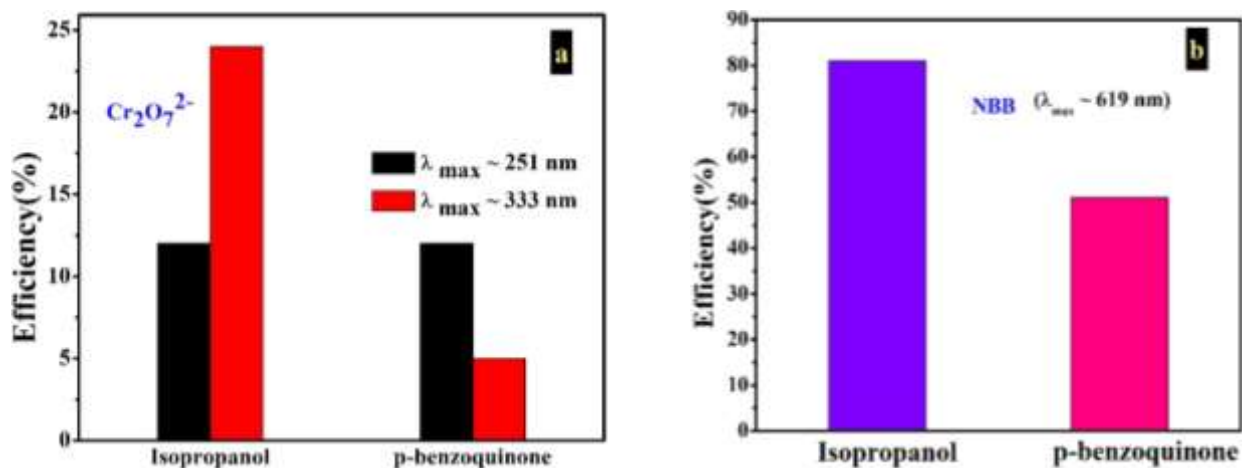


Fig. 9 Radical scavenging study on *nano* SnO₂ nanoparticles using mixture of K₂Cr₂O₇ as chromium (VI) source and Naphthol blue black Cr (VI) and NBB Degradation efficiency (a) Cr₂O₇²⁻ ($\lambda \sim 251 \text{ nm}$) and ($\lambda \sim 333 \text{ nm}$) (b) NBB ($\lambda \sim 619 \text{ nm}$) at room temperature.

Additional experiments were carried out to find out the role of reactive species involved the photocatalytic reaction with scavengers such as, isopropanol (60 $\mu\text{L molL}^{-1}$) as the hydroxyl ($\cdot\text{OH}$) radical scavenger, and p-benzoquinone (0.108 g molL^{-1}) as the superoxide ($\cdot\text{O}_2^-$) scavenger. **Fig. 9** revealed that the photocatalytic conversion of Cr (III) ions decreased from 26 % into 12 % ($\lambda \sim 251 \text{ nm}$), 41 % to 24 % ($\lambda \sim 333 \text{ nm}$) and degradation dye reduced 93 % to 81 % after addition of isopropanol. In addition, the conversion further reduced 26 % into 12 % ($\lambda \sim 251 \text{ nm}$), 41 % to 5 % ($\lambda \sim 333 \text{ nm}$) and also degradation dye reduced 93 % to 51 % after addition of benzoquinone respectively. This result shown that both charge carriers and reactive radicals are responsible by the same extent for photocatalytic degradation of mixture on tin oxide nanoparticles [26].

Conclusion

In summary, tin oxide nanoparticles were prepared by a simple facile co-precipitation method and exhibited much superior degradation and conversion of Cr (III) behavior towards degradation of mixtures (K₂Cr₂O₇ + NBB). The synergetic effect of mixture on varied concentration, quantity of catalyst, pH, and intensity of light source were optimum and investigated in detail. The catalytic conversion of Cr (III) and degradation of Naphthol blue black observed maximum efficiency at pH 5 with 100mg/100mL under ultraviolet irradiation. In photocatalytic reaction, significance of reactive species using different radical scavengers were studied in the ultraviolet irradiation to degrade mixture of K₂Cr₂O₇ and NBB.

Supplementary information

The supporting information for this articles presented degradation efficiency of content table on Cr₂O₇²⁻ ions and Naphthol blue black from the mixture (K₂Cr₂O₇+ NBB) on *nano* SnO₂ by varying parameters.

Acknowledgment

KA records his sincere thanks to the Council of Scientific and Industrial Research-HRDG (EMR Division, No. 01(2953)/18/EMR-II/1.5.2018), New Delhi, for financial support through major research project. The authors thank CIF, Pondicherry University for providing instrumental facility.

Supplementary Information

Table 1 Time dependent photodegradation efficiency data of Cr₂O₇²⁻ ions ($\lambda \sim 251 \text{ nm}$) from the mixture (K₂Cr₂O₇+ NBB) on *nano* SnO₂ by varying parameters at room temperature

Reaction Conditions		Time (min)				
		0	5	10	20	30
		Degradation efficiency of Cr ₂ O ₇ ²⁻ ions ($\lambda \sim 251 \text{ nm}$) (%)				
No catalyst		0	5	7	11	12
Surface adsorption		0	4	5	7	7
Effect of concentration	1.699 x 10 ⁻⁴ M	0	17	24	24	26
	2.832 x 10 ⁻⁴ M	0	37	37	39	39
Effect of Dosage	50 mg/100 mL	0	9	9	10	13
	75 mg/100 mL	0	12	14	16	19
	100 mg/100 mL	0	17	24	24	26
Effect of pH	pH 3	0	14	14	17	17

	pH 5	0	17	24	24	26
	pH 7	0	2	3	6	9
Intensity of light	254 nm	0	17	24	24	26
sources	365 nm	0	8	9	10	13

Table 2 Time dependent photodegradation efficiency data of $\text{Cr}_2\text{O}_7^{2-}$ ions ($\lambda \sim 333$ nm) from the mixture ($\text{K}_2\text{Cr}_2\text{O}_7 + \text{NBB}$) on *nano* SnO_2 by varying parameters at room temperature

Reaction Conditions		Time (min)				
		0	5	10	20	30
		Degradation efficiency of $\text{Cr}_2\text{O}_7^{2-}$ ions ($\lambda \sim 333$ nm) (%)				
No catalyst		0	1	1.5	3	4
Surface adsorption		0	22	22	23	26
Effect of concentration	1.699×10^{-4} M	0	35	38	40	41
	2.832×10^{-4} M	0	21	21	23	23
Effect of Dosage	50 mg/100 mL	0	22	23	25	27
	70 mg/100 mL	0	27	30	33	34
	100 mg/100 mL	0	35	38	40	41
Effect of pH	pH 3	0	31	32	34	34
	pH 5	0	35	38	40	41
	pH 7	0	5	8	12	19
Intensity of light sources	254 nm	0	35	38	40	41
	365 nm	0	26	29	30	32

Table 3 Time dependent photodegradation efficiency of Naphthol blue black ($\lambda \sim 619$ nm) from the mixture ($\text{K}_2\text{Cr}_2\text{O}_7 + \text{NBB}$) on *nano* SnO_2 by varying parameters at room temperature.

Reaction Conditions		Time (min)				
		0	5	10	20	30
		Degradation efficiency of NBB ($\lambda \sim 619$ nm) (%)				
No catalyst		0	6	7	10	11
Surface adsorption		0	66	70	72	73
Effect of concentration	2.703×10^{-5} M	0	87	91	93	93
	5.406×10^{-5} M	0	79	80	80	82
Effect of Dosage	50 mg/100 mL	0	63	67	74	79
	75 mg/100 mL	0	75	81	88	91
	100 mg/100 mL	0	87	91	93	93
Effect of pH	pH 3	0	86	88	91	92
	pH 5	0	87	91	93	93
	pH 7	0	2	2	10	12
Intensity of light sources	254 nm	0	87	91	93	93
	365 nm	0	78	83	84	85

References

- [1] Shikha Dubey, Sushmita Banerjee, Siddh Nath Upadhyay, Yogesh Chandra Sharma., Application of common nano-materials for removal of selected metallic species from water and wastewaters: A critical review., *Journal of Molecular Liquids* 240 (2017) 656–677.
- [2] Juan Jtesta, marià a. grella marta i.litter., Heterogeneous Photocatalytic Reduction of Chromium(VI) over TiO₂ Particles in the Presence of Oxalate: Involvement of Cr(V) Species, *Environ. Sci. Technol.* 2004, 38, 1589-1594.
- [3] G. Velegraki, J. Miao, C. Drivas, B. Liu, G.S. Armatas, Fabrication of 3D mesoporous networks of assembled CoO nanoparticles for efficient photocatalytic reduction of aqueous Cr(VI), *Appl. Catal. B-Environ.* 221(2018) 635–644.
- [4] H. Dong, Y. Zeng, G. Zeng, D. Huang, Y. Wu, EDDS-assisted reduction of Cr (VI) by nanoscale zero-valent iron, *Sep. Purif. Technol.* 165 (2016) 86–91.
- [5] Jin Luo, Maria Hepel ., Photoelectrochemical degradation of naphthol blue black diazo dye on WO₃ film electrode *Electrochimica Acta* 46 (2001) 2913–2922.
- [6] Hamza Ferkous, Oualid Hamdaoui, Slimane Merouani., Sonochemical degradation of naphthol blue black in water: Effect of operating parameters, *Ultrasonics Sonochemistry* 26 (2015) 40–47.
- [7] Baibai Liu , Xinjuan Liu , Mengying Ni , Chengjie Feng , Xue Lei , Can Li , Yinyan Gong , Lengyuan Niu , Jinliang Li , Likun Pan., SnO₂ as co-catalyst for enhanced visible light photocatalytic activity of Bi₂MoO₆, *Applied Surface Science* 453 (2018) 280–287.
- [8] G. Zhang, D. Chen, N. Li, Q. Xu, H. Li, J. He, J. Lu, SnS₂/SnO₂ heterostructured nanosheet arrays grown on carbon cloth for efficient photocatalytic reduction of Cr(VI), *J. Colloid Interface Sci.* 514 (2018) 306–315.
- [9] Hui Liu, Tingting Liu, Zhiling Zhang, Xiaonan Dong, Yao Liu, Zhenfeng Zhu., Simultaneous conversion of organic dye and Cr(VI) by SnO₂/rGO microcomposites, *Journal of Molecular Catalysis A: Chemical* 410 (2015) 41–48.
- [10] J. Li, T. Peng, Y. Zhang, C. Zhou, A. Zhu, Polyaniline modified SnO₂ nanoparticles for efficient photocatalytic reduction of aqueous Cr(VI) under visible light, *Separation and Purification Technology* (2018), doi: <https://doi.org/10.1016/j.seppur.2018.03.010>
- [11] Rui Fang , Ying Liang , Xueping Ge , Ming Du , Shubiao Li, Tianyu Li, Zhi Li., Preparation and photocatalytic degradation activity of TiO₂/rGO/polymer composites., *Colloid Polym Sci* (2015) 293:1151–1157.
- [12] Hui Liu n, Tingting Liu, Xiaonan Dong, Yuwu Lv, Zhenfeng Zhu., A novel fabrication of SnO₂@graphene oxide core/shell structures with enhanced visible photocatalytic activity., *Materials Letters* 126 (2014) 36–38.
- [13] D. Venkatesh, S. Pavalamalar, K. Anbalagan., Photocatalytic, Gas-Sensing and Double Layer Capacitance Properties of Nanoscale SnO₂ obtained from Template free Solution Phase Synthesis., *Journal of Materials Science: Materials in Electronics* (Submitted).
- [14] Guanglu Shang, Jihuai Wu, Miaoliang Huang, Jianming Lin, Zhang Lan, Yunfang Huang, and Leqing Fan., Facile Synthesis of Mesoporous Tin Oxide Spheres and Their Applications in Dye-Sensitized Solar Cells, *J. Phys. Chem. C* 2012, 116, 20140–20145
- [15] Jae-Hun Kim, Akash Katoch, Soo-Hyun Kim, and Sang Sub Kim., Chemiresistive Sensing Behavior of SnO₂ (n)-Cu₂O(p) Core-Shell Nanowires, *ACS Appl. Mater. Interfaces* 2015, 7, 15351–15358.
- [16] Yong Yang, Guozhong Wang, Quan Deng, Dickon H. L. Ng, and Huijun Zhao., Microwave-Assisted Fabrication of Nanoparticulate TiO₂ Microspheres for Synergistic Photocatalytic Removal of Cr(VI) and Methyl Orange, *ACS Appl. Mater. Interfaces* 2014, 6, 3008–3015.
- [17] Azam Khan, Umair Alam, Danish Ali, and M. Muneer., Visible-Light Induced Simultaneous Oxidation of Methyl Orange and Reduction of Cr(VI) with Fe(III)-Grafted K₂Ti₆O₁₃ Photocatalyst, *ChemistrySelect* 2018, 3, 7906 – 7912
- [18] Kim, K., Choi, W. Enhanced redox conversion of chromate and arsenite in ice. *Environ. Sci. Technol.* 2011, 45 (6), 2202–2208.
- [19] Ning Li, Yu Tian, Jianhui Zhao, Jian Zhang, Jun Zhang, Wei Zuo, Yi Ding, Efficient removal of chromium from water by Mn₃O₄@ZnO/Mn₃O₄ composite under simulated sunlight irradiation: Synergy of photocatalytic reduction and adsorption, *Applied Catalysis B, Environmental* <http://dx.doi.org/10.1016/j.apcatb.2017.05.041>.
- [20] G. Huang, R. Shi, Y. Zhu, Photocatalytic activity and photoelectric performance enhancement for ZnWO₄ by fluorine substitution, *J. Mol. Catal. A Chem.* 348 (2011) 100–105.
- [21] Yeoseon Choi, Min Seok Koo, Alok D. Bokare, Dong-hyo Kim, Detlef W. Bahnemann, and Wonyong Choi, Sequential Process Combination of Photocatalytic Oxidation and Dark Reduction for the Removal of Organic Pollutants and Cr(VI) using Ag/TiO₂.
- [22] Sun, B.; Reddy, E. P.; Smirniotis, P. G. Visible light Cr (VI) reduction and organic chemical oxidation by TiO₂ photocatalysis. *Environ. Sci. Technol.* 2005, 39 (16), 6251–6259.
- [23] Ning Li , Yu Tiana, Jianhui Zhao, Jian Zhang, Jun Zhang, Wei Zuo, Yi Ding, Efficient removal of chromium from water by Mn₃O₄@ZnO/Mn₃O₄ composite under simulated sunlight irradiation: Synergy of photocatalytic reduction and adsorption, *Applied Catalysis B: Environmental* 214 (2017) 126–136.
- [24] Rashmi Acharya, Brundabana Naik and Kulamani Parida., Cr (VI) remediation from aqueous environment through modified-TiO₂-mediated photocatalytic reduction, *Beilstein J. Nanotechnol.* 2018, 9, 1448–1470.
- [25] Lingyu Tian, Kelei Sun, Yulan Rui, Wenquan Cui and Weijia An., Facile synthesis of an Ag@AgBr nanoparticle decorated K₄Nb₆O₁₇ photocatalyst with improved photocatalytic properties, *RSC Adv.*, 2018, 8, 29309–29320.
- [26] Jianxing Bao, Shenghui Guo, Jiyun Gao, Tu Hu, Li Yang, Chenhui Liu, Jinhui Peng and Caiyi Jiang, Synthesis of Ag₂CO₃/Bi₂WO₆ heterojunctions with enhanced photocatalytic activity and cycling stability., *RSC Adv.*, 2015, DOI: 10.1039/C5RA18938A.